Sudan University of Science and Technology

College of Graduate Studies

Ground Observations Of Earth's Magnetic Field to Reveal the Screening Effect of the Ionosphere on Geomagnetic Pulsation

رصد المجال المغناطيسي للأرض للكشف عن تأثير طبقة الغلاف الأيوني على النبضات المغناطيسية الأرضية

A Thesis Submitted in Partial Fulfillment of the Requirements for the Degree of master in physics

Submitted by:

SABAH AHMED ALSHREEF ABASS.

Supervisor:

Dr. MAGDI ELFADIL YOUSIF SULIMAN.

July, 2019

DEDICATION

This thesis is dedicated to my parents, beloved brothers and sisters. To all my family, the symbol of love, my friends who encourage and support me, all people in my life who touched my heart, to them all I dedicate this work.

ACKNOWLEDGMENT

First I would like to thank my supervisor, Dr. MAGDI ELFADIL YOUSIF, for all help and tips I got while working on the thesis. I would also like to thank my friends and family for their love and support, without which this accomplishment would not have been achievable.

ABSTRACT

Ultra-Low Frequency (ULF) waves are plasma waves originate in upstream region of the solar wind encountering earth's magnetic field obstacle. These waves propagate through earth's magnetosphere to the ground surface of the earth passing by the ionosphere. However, upstream waves include Pc3-4 frequency range: 7-100 mHz. Accordingly, the ionosphere plays a role in characteristics of these waves that recorded on the ground. This dissertation addresses the effect of the ionosphere on the ULF waves. Here, a simultaneous ground and in situ satellite observations are carried out to detect ULF waves. In situ satellite data were obtained from the space flight mission Cluster; and the signatures of these waves were then observed on data from the ground geomagnetic station (KAG) which belong to the magnetic data acquisition system (MAGDAS) global network of magnetometers. Dynamic spectrum magnetograms of these data have shown corresponding enhancements of Pc3-4 waves amplitudes in both in situ and ground data. The waves in the source at geospace were found to be in the azimuth direction, i.e. in the By component of the data, i.e. (Toroidal) ULF mode; while their corresponding signatures on the ground were observed in the H component of the magnetic data from KAG station. These results reveal the screening effect played by the ionosphere on these ULF waves.

المستخلص

موجات التردد المنخفض للغاية (ULF) هي موجات بلازما تنشأ في منطقة المنبع من الريح الشمسية التي تواجه عقبة المجال المغناطيسي للأرض. تنتشر هذه الموجات من خلال الغلاف المغناطيسي للأرض إلى سطح الأرض للأرض والتي تمر عبر الأيونوسفير. ومع ذلك ، تشمل موجات المنبع نطاق التردد 1-100 mHz :Pc3-4 وفقًا لذلك ، يلعب الأيونوسفير دورًا في خصائص هذه الموجات المسجلة على الأرض. تتناول هذه الرسالة تأثير الأيونوسفير على موجات ULF ، هنا ، تُجرى عمليات رصد متزامنة للأرض وفي الموقع لاستكشاف موجات ULF.وقد تم الحصول على بيانات الأقمار الصناعية في موقع الفضاء من مهمة الرحلة الفضائية Cluster؛ ثم تمت ملاحظة تواقيع هذه الموجات على بيانات من المحطة المغنطيسية الأرضية الأرضية (KAG) والتي تنتمي إلى شبكة المقاييس المغناطيسية لنظام الحصول على البيانات المغناطيسية (MAGDAS)؛ وقد أظهرت الصور المغناطيسية للطيف الديناميكي لهذه البيانات تحسينات مقابلة لسعات موجات Pc3-4 في كل من بيانات الموقع والأرض. تم العثور على الموجات الموجودة في المصدر في الفضاء الجغرافي في اتجاه السمت، أي في المكون B_y حسب البيانات، أي وضع ULF (Toroidal)؛ بينما لوحظت تواقيعها المقابلة على الأرض في المكون H من البيانات المغناطيسية من محطة KAG. تكشف هذه النتائج عن تأثير الإنتقاء والذي تلعبه طبقات الأيونوسفير على موجات ULF تلك.

LIST OF FIGURES

LIST OF TABLES

LIST OF APPENDICES

List of abbreviations

no	Abbreviations	Page no
1	**ULF -** Ultra-Low Frequency	1
2	**MHD-**magneto-hydrodynamic	8
3	**FFT-**fast Fourier transforms	2
4	**IMF-**interplanetary magnetic field	9
5	**FAC-**field-aligned currents	10
6	**IAGA-**international Association of geomagnetic and Aeronomy	13
7	**HF-**high frequency	14
8	**KHI-**Kelvin-Helmholtz instability	13
9	**GPS-**global position system	14
10	**FLR-** field line resonances	15
11	IAR-ionospheric Alfvén resonator	15
12	**KAG-**Kagoshima	17
13	**UV-**Ultra violet Radiation	10
14	**MAGDAS-** MAGnetic Data Acquisition System	17

Table of Contents

CHAPTER I

INTRODUCTION

1.1 Preface to the dissertation

Ultra-Low Frequency (ULF) pulsations have been extensively studies in previous studies, because of their role as a diagnostic probe to the magnetosphere. And it is well known that conditions of the dynamic magnetosphere have impact on space-born and ground technological systems. The mechanisms of ULF waves have been investigated and there are main two mechanisms sources of these ULF waves, i.e. external solar wind driven ULF waves and internal magnetospheric processes driven ULF waves.

The ionosphere is an ionized layer within the atmosphere. And it has been known as the layer that exists in sufficient proportion as to affect the propagation of the radio waves. Therefore, ULF waves affect on the ionosphere as well as they also can be affected by the ionosphere. Study of the effect of ionosphere on ULF waves is of great importance because we can then understand well their exact role to probe the magnetosphere although their observation can be done via ground-based devices.

Moreover, it has been recognized that measuring eigenfrequencies of ULF waves is useful in remote sensing magnetospheric mass densities of populations of free charges, e.g. (Waters, et al., 2006). And in addition to estimating mass density it is possible to estimate Alfvén speed required to explain the measured travel time of MHD waves through the magnetosphere to the ground. Hence, magnetoseismology offers the ability to remotely monitor magnetospheric properties including the magnetopause location, the radial density distribution, and the plasma composition (Menk & Waters, 2011).

In this dissertation we focused on studying this effect of the ionosphere on geomagnetic ULF pulsations using magnetic data as to verify the effect as been described theoretically by many authors in their previous studies.

1.2 Statement of the research Problem

Recognizing external sources of ULF waves one can envisage the role that played by the ionosphere on these waves. That is, ULF waves have magnetic signatures on the ground and can be observed as ULF pulsations. The role of the ionosphere on

these ULF waves has been a question addressed by many authors. However, ULF pulsations play a major role in efforts towards obtaining a remotely sense tool of charges mass densities on the upper magnetosphere. Verifying the role of ionosphere is the main task will be addressed in this work.

1.3 Objectives of the research

This study aims on using ground observation of earth's magnetic field to reveal interpretation of the screening effect of the ionosphere on geomagnetic pulsation; therefore a focus is put forward on specific objectives as follows:

I. To observe magnetospheric ULF pulsations that are potentially detectable on the ground, in order to interpret the role of the ionosphere on these pulsations.
II. To verify the ground magnetic signatures of magnetospheric ULF waves.
III. To obtain suitable magnetograms required for ULF analysis using the suitable available candidate data.

1.4 Research methodology

The methodology followed is to analyze time series data of magnetic fields obtained from both satellites and ground magnetometers. The analysis is to get dynamic magnetograms via calculating the power spectrum density using fast Fourier transforms (FFT) technique in the MATLAB function 'specgram'. The range of the frequency used is in the range Pc3-4 of the Ultra-low-frequency (ULF) magnetohydrodynamic waves. Obtained magnetograms will be checked for the enhancement of amplitudes of theses waves in order to extract those waves driven by the upstream solar wind, and that are possible to be received in the ground.

1.5 Outline of the dissertation

This dissertation is constructed into four chapters. In chapter one a general introduction to the dissertation is presented, chapter two was dedicated for a theoretical background and the literature reviewing, where a brief text on plasma and space plasma is introduced, in addition an overview on ultra low frequency (ULF) in the magnetosphere is presented too, chapter three is dedicated for the methodology and data collection, and finally in chapter four results, discussion and conclusion with the recommendations is presented in this final chapter. The dissertation main chapters are followed by appendices, i.e. appendix 1 show a MATLAB code written as to obtain

magnetograms from satellite data, while appendix 2 shows a MATLAB code written as to obtain magnetograms from ground data.

CHAPTER II

THEORETICAL BACKGROUND AND THE LITERATURE REVIEW

2. 1. Introduction

The universe is made of 69 % dark energy, 27 % dark matter, and 1 % normal matter. All that we can see in the sky is the part of normal matter that is in the plasma state, and that compose 99 % of this seen part of the universe (Chen, 2016). Plasma is an "ionized" gas in which at least one of the electrons in an atom has been stripped free, leaving a positively charged nucleus, called ion. Plasma is the fourth state of matter. When a solid is heated, it becomes a liquid. Heating a liquid turns it into a gas. Upon further heating, the gas is ionized into plasma. Since a plasma is made of ions and electrons, which are charged, electric fields are rampant everywhere, Plasma usually exists only in a vacuum. Otherwise, air will cool the plasma so that the ions and electrons will recombine into normal neutral atoms. We live in a small part of the universe where plasmas do not occur naturally, otherwise, we would not be alive.

2. 2. Elementary concepts on plasma physics

Within the context that plasma is an ionized gas It is not possible that every ionized gas is plasma the reason for this can be seen from the famous Saha equation, which tells us the amount of ionization to be expected in a gas in thermal equilibrium:

$$n_i/n_n = 2.4 \times 10^5 \frac{T^{3/2}}{n_i} e^{-eU_i/kT} \quad \text{---------- (2.1)}$$

Where: n_i and n_n are respectively: the density (number per m^3) of ionized atoms and of neutral atoms, T is the gas temperature in K, k is Boltzmann's constant, U_i is the ionization energy of the gas, i.e., the number of joules required to remove the outermost electron from an atom. So plasma is a quasineutral gas of charged and neutral particles which exhibits collective behavior.

Let us consider the effect on each other of two slightly charged regions of plasma separated by a distance r . The Coulomb force between A and B diminishes as $1/r^2$. However, for a given solid angle (that is, $\Delta r/r = constant$), the volume of plasma in B that can affect A increases as r^3. Therefore, elements of plasma exert a force on one

another even at large distances. It is this long-ranged Coulomb force that gives the plasma a large repertoire of possible motions. Figure 2. 7.

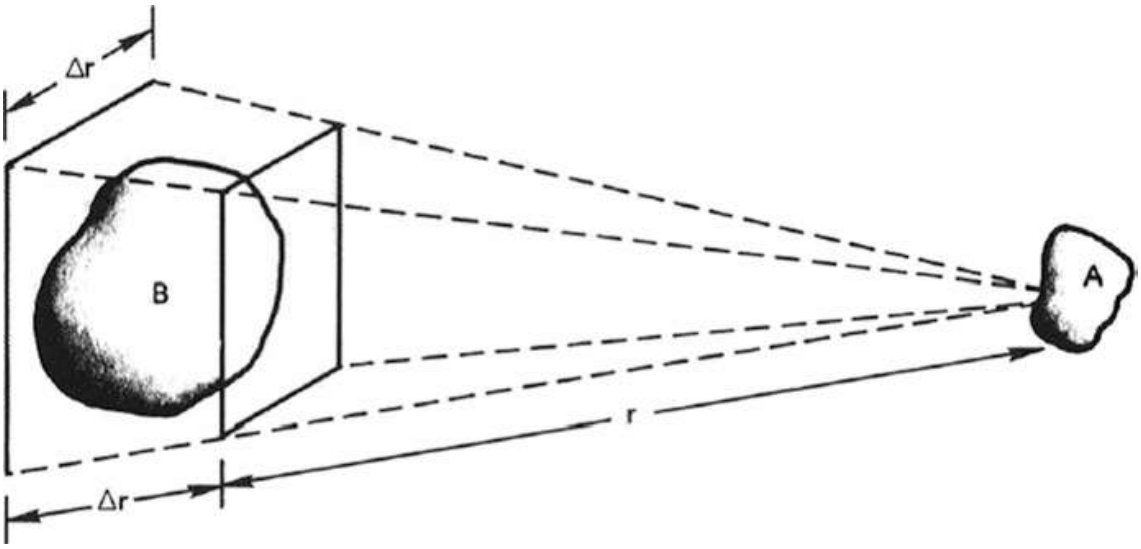

Figure 2. 7 Illustrating the long range of electrostatic forces in plasma (Chen, 2016)

Plasma seems to be a misnomer. It comes from the Greek πλάσμα,-ατος, το, which means something molded or fabricated. Because of collective behavior, plasma does not tend to conform to external influences; rather, it often behaves as if it had a mind of its own. Collective behavior means motions that depend not only on local conditions but on the state of the plasma in remote regions as well. In order to understand characteristics and behavior of plasma we need to modify our understanding to the concept of temperature.

2.2. 1. Concept of temperature:

A gas in thermal equilibrium has particles of all velocities, and the most probable distribution of these velocities is known as the Maxwellian distribution see: Figure 2. 8

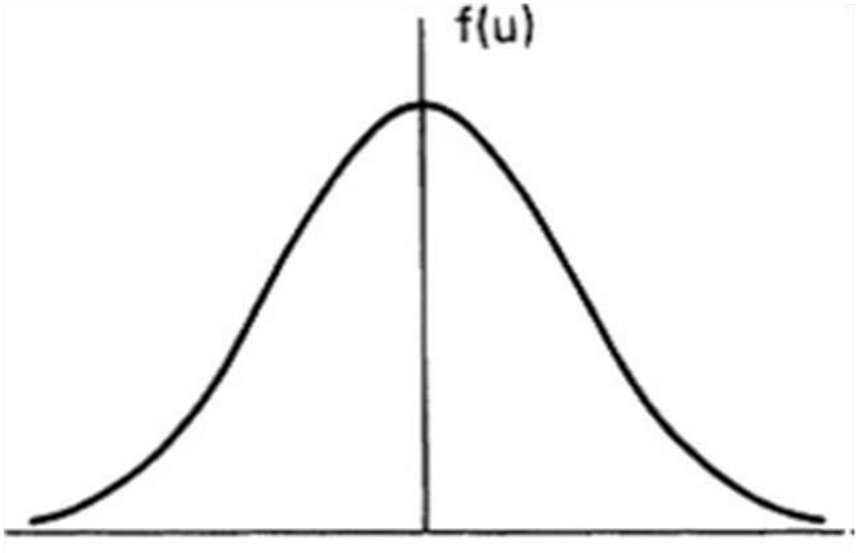

Figure 2. 8 Maxwellian velocity distribution function (Chen, 2016)

Accordingly, one can compute the average kinetic energy of particles of a system of a gas applicable to the distribution, and a relation between a temperature and energy will be obtained (Chen, 2016):

$1\ eV = 11600\ {}^{o}K$ ---------- (2.2)

It is interesting that plasma can have several temperatures at the same time. It often happens that the ions and the electrons have separate Maxwellian distributions with different temperatures T_i and T_e. This can come about because the collision rate among ions or among electrons themselves is larger than the rate of collisions between an ion and an electron. Then each species can be in its own thermal equilibrium, but the plasma may not last long enough for the two temperatures to equalize. When there is a magnetic field B, even a single species, say ions, can have two temperatures. This is because the forces acting on an ion along B are different from those acting perpendicular to B (due to the Lorentz force). The components of velocity perpendicular to B and parallel to B may then belong to different Maxwellian distributions with temperatures $T_{\perp}$ and $T_{||}$.

2.2. 2. Debye shielding

A fundamental characteristic of the behavior of plasma is its ability to shield out electric potentials that are applied to it. Suppose we tried to put an electric field inside plasma by inserting two charged balls connected to a battery. The Balls would attract

particles of the opposite charge, and almost immediately a cloud of ions would surround the negative ball and a cloud of electrons would surround the positive ball as can be seen in Figure 2.3.

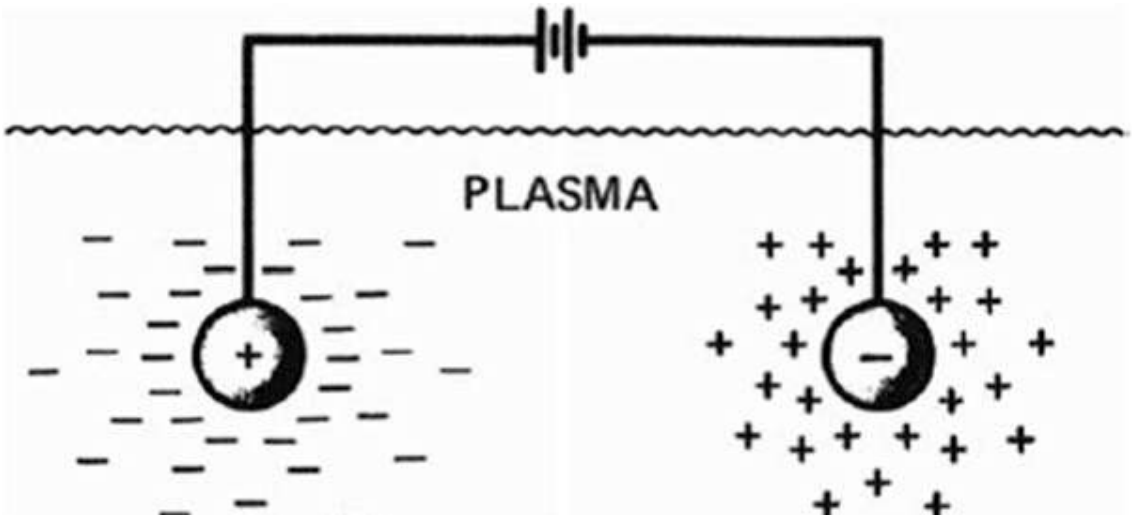

Figure 2. 9 Debye shielding

We assume that a layer of dielectric keeps the plasma from actually recombining on the surface, or that the battery is large enough to maintain the potential in spite of this. In this case we can define the Debye length to be:

$$\lambda_D = \left(\frac{\varepsilon_o K\mathrm{T}_e}{ne^2}\right)^{1/2} \quad \text{---------- (2.3)}$$

λ_D= called the Debye length, is a measure of the shielding distance or thickness of the sheath; where n stands for n_1, and $K\mathrm{T}_e$ is in joules. $K\mathrm{T}_e$ is often given in eV, in which case, we will write it also as TeV.

Which is a measure of the shielding thickness of the sheath; here the sheath is defined as the region near the grid. Hence, for ionized gas to be plasma a condition is required, i.e.

$\lambda_D \ll L$ ---------- (2.4)

2.2. 3. The plasma parameter

The picture of Debye shielding that we have given above is valid only if there are enough particles in the charge cloud. Clearly, if there are only one or two particles in the sheath region, Debye shielding would not be a statistically valid concept. We can compute the number N_D of particles in a "Debye sphere" by:

$\mathrm{N}_D = n\frac{4}{3}\pi\lambda_D^3$ ---------- (2.5)

Where: n is the density, and the product: $\Lambda = n \times \lambda_D^3$ is termed as the plasma parameter.

So in addition to the condition that $\lambda_\mathrm{D} \ll \mathrm{L}$, where L is system dimension, "collective behavior" of ionized gas that termed as plasma requires $\mathrm{N}_\mathrm{D} \gg 1$, or $\Lambda \gg 1$

2.2. 4. Criteria for plasmas

We have given two conditions that an ionized gas must satisfy to be called plasma. A third condition has to do with collisions. If ω is the frequency of typical plasma oscillations and τ is the mean time between collisions with neutral atoms, we require $\omega\tau > 1$ for the gas to behave like plasma rather than a neutral gas. The three conditions that plasma must satisfy are therefore:

1. $\lambda_D \ll L$.

2. $\mathrm{N}_D \gg 1$.

3. $\omega\tau > 1$.

2. 3. Applications of plasma physics

Plasmas can be characterized by the two parameters n and $K\mathrm{T}_e$. Plasma applications cover an extremely wide range of n and $K\mathrm{T}_e$: n varies over 28 orders of magnitude from 10^6 to $10^{34} m^3$, and $K\mathrm{T}_e$ can vary over seven orders from 0.1 to 10^6 eV. Accordingly, there are several applications of plasma in both laboratory and in nature, i.e. gas discharges (Gaseous electronics), controlled thermonuclear fusion, modern astrophysics, magneto-hydrodynamic (MHD) energy conversion and ion propulsion, solid state plasmas, gas lasers, particle accelerators, industrial plasmas, atmospherics plasmas, and space physics plasmas.

2. 4. Space plasmas

Variety of plasma population have been known to dominate space and collectively termed as space plasmas, this include sun-earth coupling system which mediate by sun plasmas and earth's geospace plasmas. The system of the magnetosphere is composed of different plasma population. And the different plasma regions in the magnetosphere can be seen from the following Figure 2. 10; which shows illustration of these plasma regions.

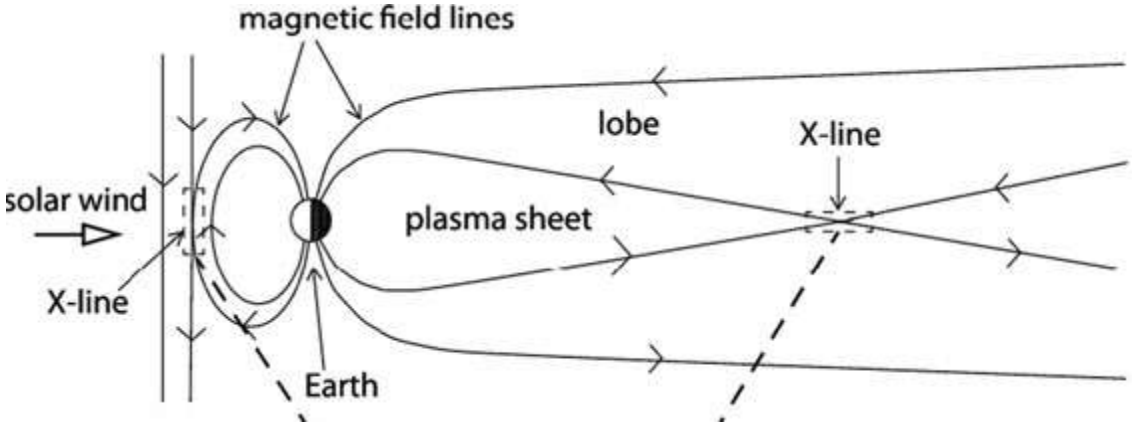

Figure 2. 10 Schematic illustration of the magnetospheric magnetic field and preferential locations of magnetic reconnection for southward IMF, i.e. at low-latitudes on the dayside (left) and in the mid-tail on the nightside (right) (Lavraud, et al., 2011).

2. 5. Structure of the inner magnetosphere

Structure of magnetosphere is as follows, and is illustrated in Figure 2. 11 which show a cross- section of the magnetosphere in the noon– midnight meridian, with north at the top and the Sun on the left. Regions of the magnetosphere are labeled in the figure. Note that the magnetic field resembles a dipole close to the Earth. The dipole region of Earth's magnetosphere is called the inner magnetosphere. On the nightside at about geosynchronous orbit (6.6 Earth radii (r_E) from the center of Earth), the magnetic field lines become stretched into a long tail-like configuration. The interaction of Earth's magnetic field with the solar wind is responsible for the distortion of its dipole field. The non-dipolar regions are called the outer magnetosphere. Immediately surrounding Earth is a region of cold (about 1 electronvolt, eV), dense (tens to thousands of particles per cm^{-3}) plasma that essentially co-rotates with Earth. This region is called the plasmasphere.

In the densest region of the magnetosphere the plasmasphere densities are billions and billions of times lower. The plasmasphere consists mostly of hydrogen and helium, but also an appreciable amount of oxygen, that have just enough energy to escape from Earth's ionosphere, the ionosphere is created by solar ultraviolet (UV) and X-ray radiation. As plasma drifts up the magnetic field line from below, it becomes trapped and co-rotates with Earth. There is often a very sharp boundary to the dense plasmasphere called the plasmapause. Often overlapping with the plasmasphere are the Van Allen two radiation belts and the ring current as can be seen in the Figure 2. 11.

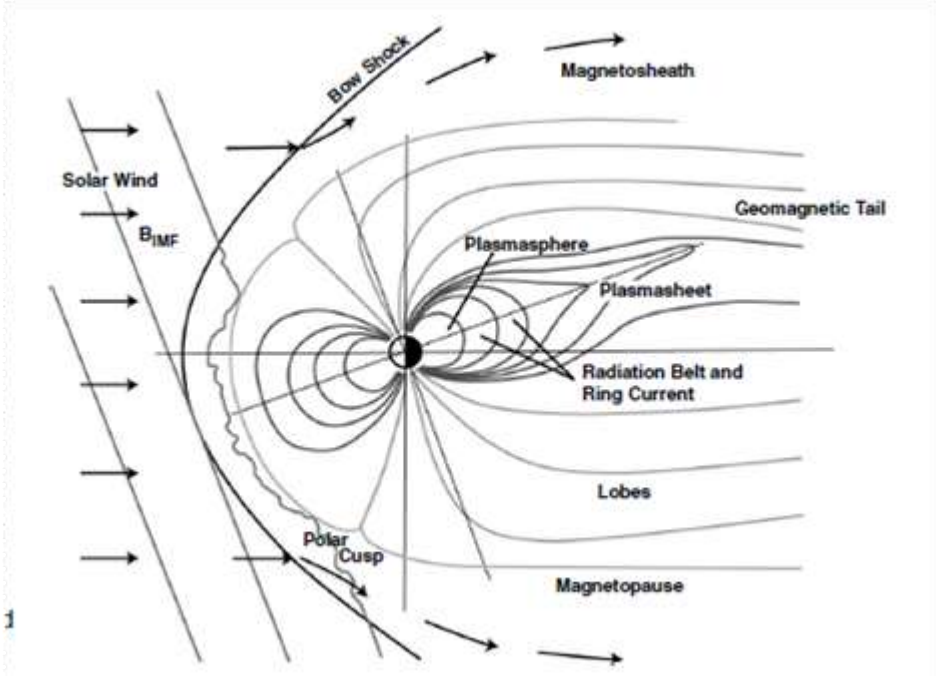

Figure 2. 11 A noon–midnight cross section of Earth's magnetosphere. Note the dipole shape of the inner magnetosphere. The Sun (hence noon) is to the left and north is up.

Moreover, in topography of the magnetosphere one can show the important current systems that are called Field-aligned currents (FAC) that connect the ring current and plasma sheet to the ionosphere. The radiation belts consist of two distinct regions of energetic particles. The outer belt, composed mostly of energetic electrons, has its inner edge around $3\,r_E$ and its highly variable outer edge usually just beyond geosynchronous orbit. The inner belt, which consists of energetic electrons and protons, extends out to about $2.5\,r_E$. These FAC play a major role in aurora and other space weather phenomena. The radiation belts contain intense radiation that can kill astronauts and damage or destroy sensitive electronics on spacecraft. Understanding this region is one of the main efforts of space weather since many important satellites have their

orbits in or through the radiation belts. The ring current is so named because its charged particles produce an electric current that encircles Earth. This magnetosphere topography showing both the noon–midnight meridian and the equatorial planecan be seen here in the following Figure 2. 12.

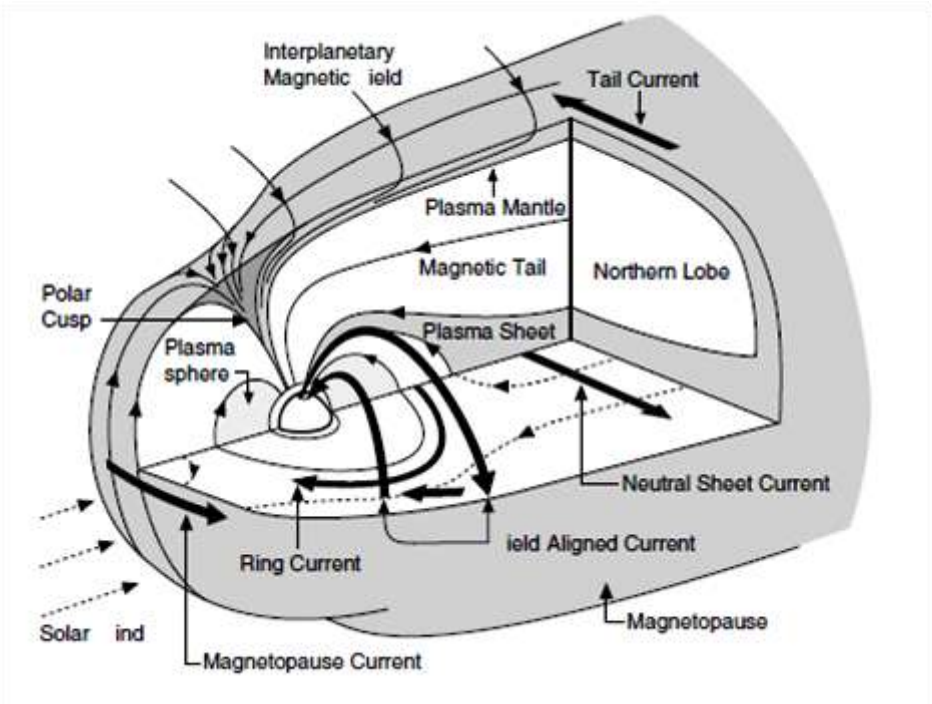

Figure 2. 12 A schematic of Earth's magnetosphere showing the equatorial and noon–midnight meridional planes. The electric currents flowing in the magnetosphere are shown as dark arrows. The regions of the magnetosphere are labeled.

2.6.ULF Waves

Ultra-low frequency (ULF) MHD plasma waves are readily recorded throughout the Earth's magnetosphere and on the ground. Generated by a variety of instabilities, ULF waves transport and couple energy throughout the system, and may play important roles in the energization and loss of radiation belt particles.ULF waves also provide a convenient probe and diagnostic monitor of the magnetosphere. Ultra-low frequency (ULF) plasma waves are broadly of two types, depending on whether their energy source originates in the solar wind or from processes within the magnetosphere (see

Table 2. 2 for more information about ULF). Evidence for the former comes from the dependence of daytime power in the $Pc3$ (20 100 mHz), $Pc4$ (7– 20 mHz) and $Pc5$ (1.7– 7 mHz) ranges on solar wind speed and interplanetary magnetic field (IMF) clock angle. Solar wind density also plays an important role in controlling Pc3 activity. Substorms and other instabilities in the tail form an important source of ULF waves on the nightside.

According to external mechanisms of these ULF, it is expected that these waves to propagate into the magnetosphere system, and the consequence is that these ULF waves shall be affected by any else part of a coupling system that may encounter the magnetosphere system, i.e. the magnetosphere- ionosphere coupling system. This is a deductable result in a simple interpretation scenario which is clarified in the following subsections.

Table 2. 2 The International Association of Geomagnetism and Aeronomy (IAGA) classification scheme for ULF ((Villante, 2007), and the references therein).

	T(s)	Frequency	Sources
Pc1 Pc2	0.2 – 5 5 – 10	High: 0.1 – 10 Hz	Ion-cyclotron instability in magnetosphere.
Pc3	10 – 45	Mid: 10 – 100 mHz	Proton-cyclotron instability in the SW; Kelvin–Helmholtz instability.
Pc4 Pc5	45 – 150 150 – 600	Low: 1 – 10 mHz	Kelvin–Helmholtz instability; Drift-mirror instability; Bounce resonance.
Pi1	1 – 40		Field aligned current driven instabilities.
Pi2	40 – 150		Abrupt changes in convection in the magnetotail; Flux transfer events.

2.6.1.Instabilities at the Magnetopause

The correlation between solar wind speed and ULF power in the magnetosphere suggests that the Kelvin- Helmholtz instability (KHI) resulting from the velocity shear at the magnetopause may be a significant source of ULF wave energy ((Menk & Waters, 2011), and the references therein).The resultant surface waves propagate anti-sunward and are strongly evanescent within the magnetosphere. However, the shear flow between the plasma in the magnetosheath and magnetosphere also controls the reflection condition at the magnetopause, and when taking into account the boundary layer thickness this may result in the formation of over-reflection modes at the magnetopause.

2.6.2.The Ionosphere Boundary

The conducting ionosphere forms the inner boundary of the magnetospheric cavity and therefore controls not only the formation and properties of standing field line oscillations. All ULF waves observed on the ground propagate through the ionosphere and are therefore affected by its properties. The best known effect is the rotation of the polarization azimuth of the down going wave. The fields of these propagating waves

can affect the ionospheric density distribution, thereby modifying ionospheric properties. These effects can be detected with HF radars and other sounders, and may modify the total electron content along the global positioning system (GPS) signal paths.

2.7.Effects of the Ionosphere on ULF Waves

MHD models now being used to investigate the effects of ionospheric conductivity on FLRs incorporate a realistic ionosphere, oblique magnetic fields, and a mixture of incident wave modes. (Menk & Waters, 2011) presented an analytic description of this form, including a reflection and wave mode conversion coefficient matrix to describe mixing and conversion between shear Alfvén and fast mode energy at the ionosphere and atmosphere. These properties were found to depend critically on the perpendicular wave number k_y. This formulation was extended by. (Menk & Waters, 2011) to include an inductive shielding effect for oblique magnetic fields (and hence high to low latitudes). This effect arises from the generation of an 'inductive' rotational current by the induced part of the divergent electric field in the ionosphere, reducing the wave amplitude detected on the ground. Using a 1-D numerical formulation, (Menk & Waters, 2011) found that for an oblique magnetic field the rotation of the wave polarization azimuth depends on the compressional mode characteristics and the mode conversion and reflection properties from the ionosphere. Waters (Menk & Waters, 2011) and described a 2-D MHD formulation which was used to investigate the dependence of FLR frequency on ionospheric conductivity. They found that under typical mid/low latitude summer and winter conditions the FLR frequencies change by less than 5%. However, at auroral latitudes it is necessary to account for ionospheric feedback arising from changes in the Pedersen conductivity due to electron precipitation. incorporated a model of an active auroral ionosphere with a 2-D MHD model of the magnetosphere using both dipolar and stretched field geometries. They found that ionospheric feedback effects can produce strongly localized FLRs and enhanced amplitudes. Direct observations of low-mid latitude Pc3-4wave structure with the CHAMP spacecraft and simultaneously on the ground below were described by (Menk & Waters, 2011). These confirm that Pc3-4 waves propagate through the magnetosphere mostly in the compressional mode and appear in the D component on the ground, coupling to discrete FLRs at the characteristic latitude, with 90◦ rotation in

polarization of the signal on the ground. This situation was confirmed by (Waters, et al., 2006) using numerical modeling to calculate the relationship between Pc3 wave power above the ionosphere and on the ground. They also found that diurnal variations in the ionosphere/ground amplitude ratio do not depend strongly on ionospheric conductance, but the fast mode field is sensitive to the crustal surface conductivity. At equatorial latitudes the nonuniform ionospheric conductivity at dawn results in strong changes in Pc3 amplitude and D component phase on the ground, although the phase of the H component is largely unchanged. It is not clear whether these results from the ionospheric affect on incident Alfvén or fast mode waves. New observations and modeling have confirmed the existence of quarter-mode FLRs near the dawn terminator, mostly in winter and summer in the US sector. These modes result from the asymmetry in ionospheric conductivity at conjugate points, and point to the need for caution in FLR-based magnetospheric density surveys. The difference in solar illumination at conjugate points also causes a strong seasonal asymmetry in plasmaspheric density that is maximum in US longitudes around L=2–3 (Waters, et al., 2006). New datasets and improvements in modeling the effect of the ionosphere are starting to provide a clear picture of the propagation of Pc3-4 signals to the ground. Consideration of ionospheric effects at Pc1 frequencies should incorporate the effect of the ionospheric Alfvén resonator (IAR). The IAR affects the spectrum of 0.1–10 Hz wave power reaching the ground (Waters, et al., 2006). And at low latitudes is expected to be excited by lightning discharges. Properties of the IAR, including the diurnal variation, are determined mainly by the variation in Alfvén velocity at the F-layer peak. (This issue) provide a detailed description of wave propagation in the IAR, pointing out the need to include magnetic inclination effects away from high latitudes. This changes the resonant frequency.

2.7.Effects of ULF Waves on the Ionosphere

ULF wave fields drive perturbations in the ionosphere that may be detected with high frequency (HF) Doppler sounders or HF radars including the low latitude Arecibo radar .Doppler sounder measurements, in particular, have revealed the existence of a significant population of very high-m waves that is largely hidden from ground magnetometers. The process by which Alfvén waves incident on and propagating through the ionosphere lead to ULF ionospheric Doppler oscillations. This was

extended and generalized by Waters et al. to incorporate a mixture of downgoing wave modes and oblique magnetic field geometry, providing good agreement with observed Doppler shifts for an m∼150 and m∼10 event recorded by HF sounders near 66◦ latitude. ULF field line signatures can be recorded in the ionosphere from low to high latitudes. The waves may arise from solar wind pressure perturbations, or be triggered by substorms. Under appropriate assumptions of horizontal wave number and mode mix of the incident waves, relatively simple models can predict the resultant amplitude and phase profile reasonably well. Extension of these models to higher dimensions would provide more information on ULF wave properties at the ionosphere. It is clear, however, that ionospheric sounders can provide new information not available from magnetometers on ULF waves at the lower boundary of the magnetosphere-ionosphere system.

2.8. Magnetospheric Remote Sensing

It has long been recognized that measurement of the eigenfrequency of magnetospheric field line resonances can provide information on the mass density threading the field line, mostly near the equatorial plane where the field-aligned Alfvén speed is a minimum. However, the distribution of plasma mass density along the field line alters the harmonic spacing of ULF resonances and mass loading due to heavy ions of ionospheric origin becomes important at low latitudes.

Magnetoseismology offers the ability to remotely monitor magnetospheric properties including the plasmapause location, the radial density profile, and under certain conditions the presence of plasma plumes, the field-aligned density distribution, and the plasma composition. Measurements of the field line eigenfrequency and harmonics are the most established techniques for this, although the wave travel time can also provide information on the density distribution. Further intercalibration studies are required to compare ground-based mass density estimates with in situ observations in order to understand the full utility of the technique, and the precision of composition estimates. It would also be interesting to study how mass loading and hence plasma composition varies with magnetic activity and L.

CHAPTER III

METHODOLOGY AND DATA COLLECTION

3.1.Data

Ground geomagnetic raw data were collected from the global network of stations of the magnetic data acquisition system (MAGDAS) project of the Kyushu University, Japan. Data in hourly span of a one day on: September 5, 2002 were used, i.e. to select the event according to (Clausen, et al., 2009).

The following Figure 3. 2 shows the MAGDAS stations worldwide.

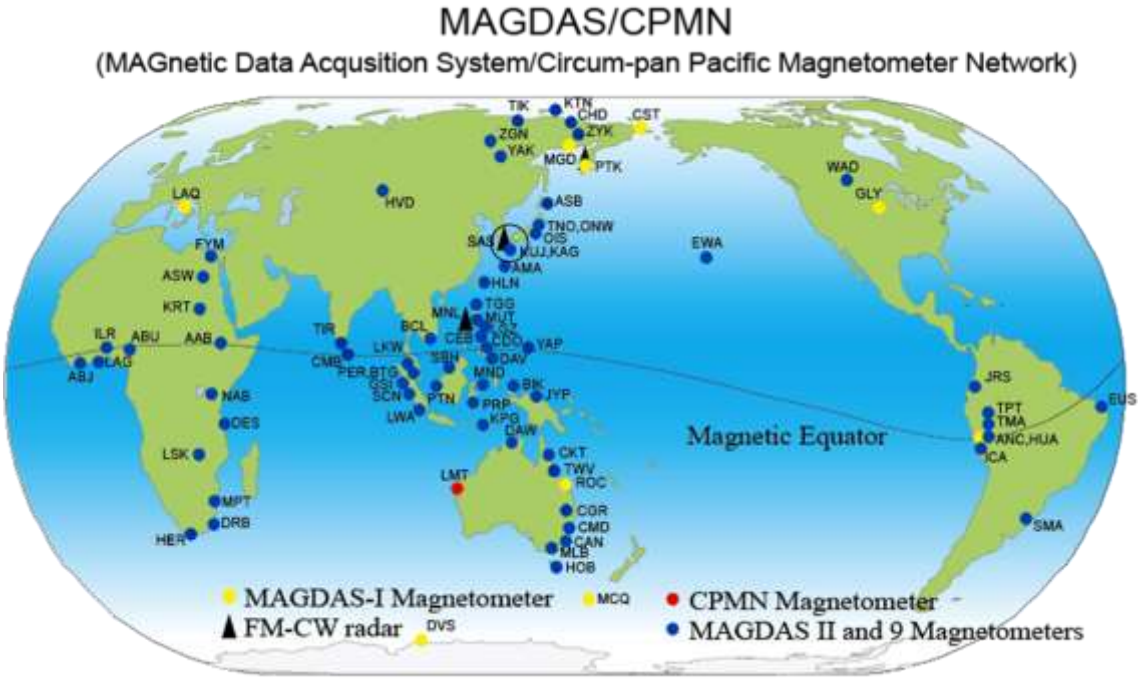

Figure 3. 2 The MAGnetic Data Acquisition System (MAGDAS) station map showing KAG station in the black circle.

On the other hand, the satellites data are obtained from Cluster satellite from the Goddard space flight center, space physics data facility, OMNI plus data webpage, (Papitashvili, 2019).

3.2.Methodology and data analysis

Magnetic data were obtained from both satellites and ground magnetometers. And using these data the dynamic magnetograms were carried out, and that is via calculating the power spectrum density using fast Fourier transforms (FFT) technique built in the MATLAB function ‘specgram’. The range of the frequency used is in the range of Pc3-4 of the Ultra-low-frequency (ULF) magnetohydrodynamic waves. Enhancement in amplitudes were checked out to select Pc3-4 events of theses ULF waves looking for solar wind driven waves in the in situ data, and also the corresponding signatures of these ULF waves on the ground in from the ground magnetic data from KAG station.

The aforementioned method was done using MATLAB codes dedicated for reading and analyzing the magnetic data from both satellite and ground data, respectively. Time series data in the time span covered in the day of September 5, 2002 were selected referring to (Clausen, et al., 2009).

CHAPTER IV

RESULTS, DISCUSSION AND CONCLUSION

4.1. Results

The following Figure 4. 2 shows Pc3-4 waves from an external driven source (satellite data), and the corresponding ground observation.

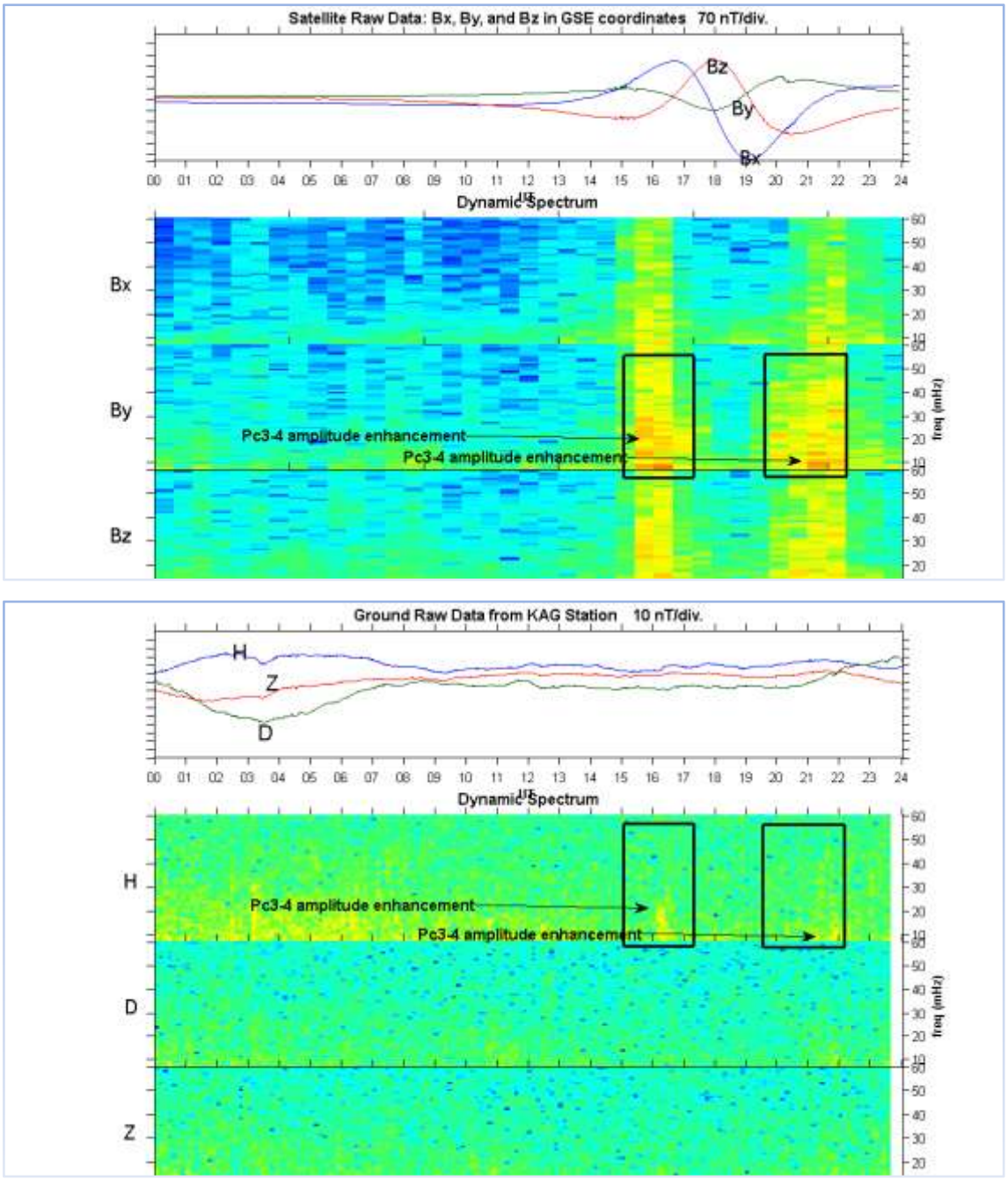

Figure 4. 2 Upper two panels show raw data of magnetic field obtained from Cluster satellites in GSE coordinates and dynamic spectrum showing a Pc3-4 event, respectively. While the lower two panels show raw data obtained from a

ground station Kagoshima (KAG) and the dynamic spectrum in the Pc3-4 showing ground observation of the same event, respectively.

4.2. Discussion

One of the mechanisms that produce ULF in the Pc3-4 range is the solar wind. And these upstream waves propagate in the magnetosphere and pass through the earth's ionosphere to the ground where their signature can be detected by magnetograms of data from ground observatories. It was found that, mainly, the ionosphere play a role as to rotate fields of these waves 90^o in the polarization direction as they propagate through it. The consequence is that whence, these observed waves are poloidal in their direction they will be received as toroidal waves on the ground and the other way around. The physics describes this is that the ionosphere is compose of free charges and electrons and therefore currents could be initiated by the fields of these waves. The obtained result, as can be found in Figure 4. 2 the magnetogram of the satellite data show a poloidal waves Pc3-4 in azimuth direction while on the ground magnetogram of data from KAG station show a corresponding signature of these waves in the H component data. The conclusion is that the ionosphere rotated fields of these upstream waves 90^o in the polarization direction.

4.3. Conclusion

In this research, upstream waves in the range of Pc3-4 were found to be 90^o rotated in their corresponding fields and polarization direction as they pass through the ionosphere, this result interpret the screening role played by the ionosphere.

4.4. Recommendations

We recommend that low- latitude ground magnetic data observations should be developed further, because of the capability of using these data in probing and investigating the whole magnetosphere.

REFERENCES

Chen, F. F., 2016. *Introduction to plasma physics and controlled fusion.* Third edition ed. Switzerland: Springer International Publishing.

Clausen, L. B. N. et al., 2009. First simultaneous measurements of waves generated at the bow shock in the solar wind, the magnetosphere and on the ground. *Annales Geophysicae,* Volume 27, pp. 357-371.

Lavraud, B., Foullon, C., Farrugia, C. J. & Eastwood, J. P., 2011. The magnetopause, its boundary layers and pathways to the magnetotail. In: *The dynamic magnetosphere.* Dordrecht: Springer, pp. 3-28.

Menk, F. W. & Waters, C. L., 2011. Magnetospheric ULF waves: A review. In: *The dynamic magnetosphere.* Dordrecht: Springer, pp. 223-256.

Papitashvili, N., 2019. *Goddard space flight center: Space Physics data facility.* [Online] Available at: https://omniweb.gsfc.nasa.gov
[Accessed 25 7 2019].

Treumann, W. B. a. R. A., 1997. *Basic Space Plasma Physics.* London: Imperial College Press.

Villante, U., 2007. Ultra Low Frequency (ULF) Waves in the Magnetosphere. In: Y. Kamide & A. C. Chian, eds. *Handbook of the solar-terrestrial environment.* 1 ed. Berlin: pringer-Verlag, pp. 396-422.

Walker, A. D. M., 2005. *Magnetohydrodynamics Waves in Geospace.* Kwazulu-Natal, South Africa: Institute of Physics (IoP) publishing Ltd.

Waters, C. et al., 2006. Remote sensing the magnetosphere using ground- based observations of ULF waves. In: *Magnetospheric ULF waves: Synthesis and new directions.* San Francisco: American Geophysical Union, pp. 319-340.

APPENDICES

Appendix 3 A MATLAB code written as to obtain magnetograms from satellite data.

```
function    Raw_Dynamic_Sat(PathName,FileName)
%
% Original program for J-format by Y-M.Tanaka@NIPR
% This file is modified for MAGDAS-storage by
S.Abe
%
% ========= Open file ======================
% rewrite the following
[~,JJJ]
=ReadSat1m('D:\Hatozi\تحميل\ClusterData\CLU\2002\CL
U20020905.TXT');
SP=1;
%JJJ=[(JJJ(:,1)-JJJ(1,1)),...
     %(JJJ(:,2)-JJJ(1,2))-10,...
     %(JJJ(:,3)-JJJ(1,3))-20];
% JJJ(:,1)=rm_noise(JJJ(:,1),5);
% JJJ(:,2)=rm_noise(JJJ(:,2),5);
% JJJ(:,3)=rm_noise(JJJ(:,3),5);
%DJ=[zeros(1,3);diff(JJJ)];
%BJ=bandpass(JJJ(:,1),SP,10,150);
JJJ(JJJ>=1000)=NaN;
JJJ(JJJ<=-1000)=NaN;
Hour=[0:SP:(21488-SP)]/900;
% ========== Make Figure 1
==================================
%h1Figure=figure('PaperUnits','normalized','PaperT
ype','a4letter','PaperOrientation','portrait','Pap
erPosition',[0 0 1
1],'Units','normalized','Position',[0.05 0.03
0.9*0.7 0.9]);

% ========== Plot Raw data
==================================
h1=axes('position',[0.15,0.73,0.75,0.22]);

XTickVector=linspace(0,24,25);
for i=1:25,

XTickTexts(i,:)=sprintf('%2.2d',XTickVector(i));
end
```

```
%--- For Color Plot ---%
plot(Hour,JJJ(:,1),Hour,JJJ(:,2),Hour,JJJ(:,3));

Nt=0;
YNo = 100;
while YNo > 15
    Nt = Nt + 10;
    YLimData=get(h1,'YLim');
    YNo=ceil((YLimData(2)-YLimData(1))/Nt);

YTickVector=linspace(YLimData(1),YLimData(1)+Nt*(Y
No-1),YNo);
end

set(h1,'XLim',[0 24],...
            'XTick',XTickVector,...
            'XTickLabel',XTickTexts,...
            'YTick',YTickVector,...
            'YTickLabel',[],...
            'tickdir','out');

XLimData=get(h1,'XLim');
text_compSat(JJJ,XLimData,YLimData,SP);
xlabel('UT','fontsize',10)
title(sprintf('Raw Data    %g nT/div.',Nt));
%text(0.5,1.2,sprintf('%4d/%2.2d/%2.2d  %s',...
%DD(1),DD(2),DD(3),ST),'Units','normalized','fonts
ize',18,'horizontalalignment','center')
text(1,1.18,'Fig.1','Units','normalized','fontsize
',10,'horizontalalignment','right')
% ========== Plot Dynamic Spectra
=================================
XTickVector=linspace(0,24,25);
str_comp=['Bx';'By';'Bz'];
for i=1:25,

XTickTexts(i,:)=sprintf('%2.2d',XTickVector(i));
end

for i=1:3
  h2=axes('position',[0.15,0.63-
i*0.22,0.75,0.22]);

    if SP==1,
```

```
        [PS,F,TS] = specgram(JJJ(:,i),1024,1/SP);
    else
        [PS,F,TS] = specgram(JJJ(:,i),512,1/SP);
    end
    pcolor(TS/3600,F*1000,real(log10(PS+eps)));
    shading flat
    %surf(TS/60,F*1000,real(log10(PS+eps)));
    %axis tight;
    %view(0,90);
    % colormap(flipud(gray))
    set(h2,'ylim',[7 60],...
           'xtick',0:24,...
           'xticklabel',[],...
           'tickdir','out',...
           'yaxislocation','right')
    text(-
0.06,0.5,str_comp(i),'Units','normalized','fontsiz
e',15)

    if  i==1,
        title(sprintf('Dynamic Spectrum'))
    end
    if  i==2,
        ylabel('freq (mHz)')
    end
end

set(h2,'Xticklabel',XTickTexts)
xlabel('UT')

%--- End of File ---%
```

Appendix 4 AMATLAB code written as to obtain magnetograms from ground data.

```
function   Raw_Dynamic(PathName,FileName)
%
% Original program for J-format by Y-M.Tanaka@NIPR
% This file is modified for MAGDAS-storage by
S.Abe
%
% ========= Open file ======================
% rewrite the following
[~,JJJ]=ReadIAGA1s('D:\Hatozi\تحميل\KAG\2002\KAG200
20905psec.SEC');
SP=1;
JJJ=[(JJJ(:,1)-JJJ(1,1)),...
     (JJJ(:,2)-JJJ(1,2))-10,...
     (JJJ(:,3)-JJJ(1,3))-20];
% JJJ(:,1)=rm_noise(JJJ(:,1),5);
% JJJ(:,2)=rm_noise(JJJ(:,2),5);
% JJJ(:,3)=rm_noise(JJJ(:,3),5);
%DJ=[zeros(1,3);diff(JJJ)];
%BJ=bandpass(JJJ(:,1),SP,10,150);
JJJ(JJJ>=1000)=NaN;
JJJ(JJJ<=-1000)=NaN;
Hour=[0:SP:(86400-SP)]/3600;
% ========== Make Figure 1
==================================
%h1Figure=figure('PaperUnits','normalized','PaperT
ype','a4letter','PaperOrientation','portrait','Pap
erPosition',[0 0 1
1],'Units','normalized','Position',[0.05 0.03
0.9*0.7 0.9]);

% ========== Plot Raw data
==================================
h1=axes('position',[0.15,0.73,0.75,0.22]);

XTickVector=linspace(0,24,25);
for i=1:25,

XTickTexts(i,:)=sprintf('%2.2d',XTickVector(i));
end

%--- For Color Plot ---%
plot(Hour,JJJ(:,1),Hour,JJJ(:,2),Hour,JJJ(:,3));
```

```
Nt=0;
YNo = 100;
while YNo > 15
    Nt = Nt + 10;
    YLimData=get(h1,'YLim');
    YNo=ceil((YLimData(2)-YLimData(1))/Nt);

YTickVector=linspace(YLimData(1),YLimData(1)+Nt*(Y
No-1),YNo);
end

set(h1,'XLim',[0 24],...
            'XTick',XTickVector,...
            'XTickLabel',XTickTexts,...
            'YTick',YTickVector,...
            'YTickLabel',[],...
            'tickdir','out');

XLimData=get(h1,'XLim');
text_comp(JJJ,XLimData,YLimData,SP);
xlabel('UT','fontsize',10)
title(sprintf('Raw Data    %g nT/div.',Nt));
%text(0.5,1.2,sprintf('%4d/%2.2d/%2.2d  %s',...
%DD(1),DD(2),DD(3),ST),'Units','normalized','fonts
ize',18,'horizontalalignment','center')
text(1,1.18,'Fig.1','Units','normalized','fontsize
',10,'horizontalalignment','right')
% ========== Plot Dynamic Spectra
==================================
XTickVector=linspace(0,24,25);
str_comp=['H';'D';'Z'];

for i=1:25,

XTickTexts(i,:)=sprintf('%2.2d',XTickVector(i));
end

for i=1:3
  h2=axes('position',[0.15,0.63-
i*0.22,0.75,0.22]);

    if SP==1,
        [PS,F,TS] = specgram(JJJ(:,i),1024,1/SP);
    else
```

```
        [PS,F,TS] = specgram(JJJ(:,i),512,1/SP);
    end
    pcolor(TS/3600,F*1000,real(log10(PS+eps)));
    shading flat
    % colormap(flipud(gray))

    set(h2,'xlim',[0 24],...
           'ylim',[7 70],...
           'xtick',0:24,...
           'xticklabel',[],...
           'tickdir','out',...
           'yaxislocation','right')
    text(-
0.04,0.5,str_comp(i),'Units','normalized','fontsiz
e',15)

    if  i==1,
        title(sprintf('Dynamic Spectrum'))
    end
    if  i==2,
        ylabel('freq (mHz)')
    end
end

set(h2,'Xticklabel',XTickTexts)
xlabel('UT')


function   text_comp(JJJ,XLimData,YLimData,SP)
%
% Write H, D, Z text in the Figure
%
JJJ_tmp=JJJ;
Jindex=[1,2,3];
Textcmp_mat=['H';'D';'Z'];

[maxrow,maxrow_index] = max(JJJ_tmp);
[maxcmp,maxcmp_index] = max(maxrow);

if  maxcmp_index==1,
    Textcmp=Textcmp_mat(1);
elseif  maxcmp_index==2,
    Textcmp=Textcmp_mat(2);
else
    Textcmp=Textcmp_mat(3);
```

```
end

Xpos=maxrow_index(maxcmp_index)*SP/3600/(XLimData(
2)-XLimData(1));
Ypos=(maxcmp-YLimData(1))/(YLimData(2)-
YLimData(1))+0.03;
text(Xpos,Ypos,Textcmp,'Units','normalized','fonts
ize',16,...
'horizontalalignment','center')

Jindex(maxcmp_index)=[];
Textcmp_mat(maxcmp_index)=[];
JJJ_tmp=JJJ_tmp(:,Jindex);

[minrow,minrow_index] = min(JJJ_tmp);
[mincmp,mincmp_index] = min(minrow);

if  mincmp_index==1,
    Textcmp=Textcmp_mat(1);
else
    Textcmp=Textcmp_mat(2);
end

Xpos=minrow_index(mincmp_index)*SP/3600/(XLimData(
2)-XLimData(1));
Ypos=(mincmp-YLimData(1))/(YLimData(2)-
YLimData(1))-0.06;
text(Xpos,Ypos,Textcmp,'Units','normalized','fonts
ize',16,...
'horizontalalignment','center')

%--- End of File ---%
```